J. Fluid Mech. (2009), *vol.* 636, *pp.* 455–474.
doi:10.1017/S0022112009990802

On the stability of shallow rivulets

E. S. BENILOV†

Department of Mathematics, University of Limerick, Limerick, Ireland

(Received 6 October 2008 and in revised form 12 June 2009)

We examine the linear stability of a capillary rivulet under the assumption that it is shallow enough to be described by the lubrication approximation. It is shown that rivulets *on* a sloping plate are stable regardless of their parameters, whereas rivulets on the *underside* of a plate can be either stable or unstable, depending on their widths and the plate's slope. For the case of a horizontal plate, sufficiently narrow rivulets are shown to be stable and sufficiently wide ones unstable, with the threshold width being $\pi/2\,(\sigma/g\rho)^{1/2}$ (ρ and σ are the liquid's density and surface tension, g is the acceleration due to gravity).

It is also shown that, even though the plate's slope induces in a rivulet a sheared flow (which would normally be viewed as a source of instability) – in the present problem, it is a stabilizing factor. The corresponding stability criterion involving the rivulet's width and the plate's slope is computed, and it is demonstrated that, if the latter is sufficiently strong, all rivulets are stable regardless of their widths.

1. Introduction

Rivulets, or shallow and narrow flows of liquid, play an important role in hydrodynamics. The seminal results on their stability was obtained by Davis (1980) and Weiland & Davis (1981), who used the linearized Navier–Stokes equations to examine the stability of normal modes. The stability of rivulets has also been studied using variational methods (Langbein 1990; Roy & Schwartz 1999) and by exploring whether or not it is energetically favourable for a rivulet to split up into several subrivulets (e.g. Schmuki & Laso 1990; Myers, Liang & Wetton 2004; Wilson & Duffy 2005; Sullivan, Wilson & Duffy 2008).

Note also that almost all of the above papers dealt with rivulets *on* a rigid plate. The only exception is the work of Sullivan *et al.* (2008), who examined the stability of rivulets on the *underside* of a plate (which are, obviously, much more unstable due to the effect of 'inverted' gravity). Their analysis, however, was restricted to liquids/substrates that do not exhibit the so-called hysteresis of contact angles.

In the present paper, we consider the case where the liquid–substrate interaction involves a finite-width hysteresis interval. Rivulets are assumed to be sufficiently shallow and, thus, satisfy the lubrication approximation; their stability is examined through the usual linear stability approach based on normal modes. In § 2, we shall examine the stability of a rivulet on a sloping plate and compare the results to those obtained previously. Rivulets on the underside of a plate are examined in § 3.

† Email address for correspondence: eugene.benilov@ul.ie

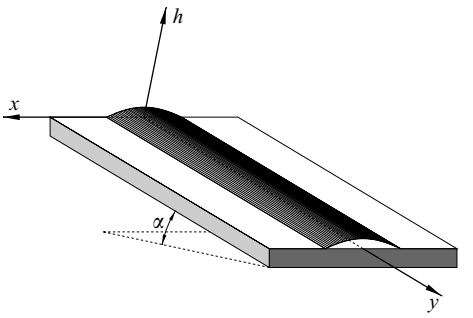

FIGURE 1. The setting: a rivulet on a sloping plate.

2. Rivulets on a plate

2.1. *Mathematical formulation*

Consider a layer of liquid (of density ρ, kinematic viscosity ν, surface tension σ) on a plate inclined at an angle α to the horizontal (see figure 1). The depth h of the layer depends on the time t and the spatial coordinates (x, y); the y-axis is directed along the direction of the fastest slope.

Assume also that the layer is shallow, the slope of its (free) surface is close to that of the plate, and the Reynolds number of the flow is small. In this case, the lubrication approximation can be used, yielding the following asymptotic equation:

$$\frac{\partial h}{\partial t}+\frac{g\,\sin\alpha}{\nu}\frac{\partial}{\partial y}\left(\frac{h^3}{3}+\lambda h^2\right)+\nabla\cdot\left[\left(\frac{h^3}{3}+\lambda h^2\right)\nabla\left(\frac{\sigma}{\rho\nu}\nabla^2 h-\frac{g\,\cos\alpha}{\nu}h\right)\right]=0, \quad (2.1)$$

where g is the acceleration due to gravity and λ is the so-called slip length (introduced to relax the no-slip condition near the contact lines). The term involving $g\,\sin\alpha$ describes the down-the-slope acceleration, the one with $g\,\cos\alpha$ describes the hydrostatic pressure gradient due to variations of the rivulet's depth, and the one with σ, surface tension.

The derivation of (2.1) will not be presented here, as it is very similar to that of its two-dimensional counterpart derived by Hocking (1981). Note also that if the flow did not involve contact lines, or even if it did but they were not moving, the terms including λ could be omitted – after which (2.1) would coincide with an equation derived by Bertozzi & Brenner (1997).

Now, introduce the following non-dimensional variables:

$$x_*=\frac{x}{L_c}, \qquad y_*=\frac{y}{L_c}, \qquad t_*=\frac{\sigma H^3 t}{\rho\nu L_c^4}, \qquad h_*=\frac{h}{H}, \quad (2.2)$$

where H will later be identified with the maximum depth of the rivulet, and

$$L_c=\sqrt{\frac{\sigma}{\rho g\,\cos\alpha}} \quad (2.3)$$

is the capillary scale. Observe that, for $\alpha=90^\circ$ (vertical plate), L_c becomes infinite and the problem should be non-dimensionalized differently. It will be shown, however, that all rivulets are stable in this case and it is, thus, unimportant.

Substituting (2.2)–(2.3) into (2.1) and omitting the asterisks, we obtain

$$\frac{\partial h}{\partial t}+\gamma\frac{\partial}{\partial y}\left(\frac{h^3}{3}+\mu h^2\right)+\nabla\cdot\left[\left(\frac{h^3}{3}+\mu h^2\right)\nabla\left(\nabla^2 h-h\right)\right]=0, \quad (2.4)$$

where

$$\gamma = \frac{L_c \tan\alpha}{H}, \qquad \mu = \frac{\lambda}{H}. \tag{2.5}$$

are the normalized slope of the plate and non-dimensional slip length.

Next we need to formulate boundary conditions at the contact lines. Let these be located at $x = x_\pm(y, t)$, which implies

$$h \to 0 \qquad \text{as} \qquad x \to x_\pm. \tag{2.6}$$

We shall also require the normal component of the mass flux at the contact lines be zero,

$$\boldsymbol{n}_\pm \cdot \left[\gamma\left(\frac{h^3}{3} + \mu h^2\right)\boldsymbol{e}_y + \left(\frac{h^3}{3} + \mu h^2\right)\nabla\left(\nabla^2 h - 1\right)\right] \to 0 \qquad \text{as} \qquad x \to x_\pm, \tag{2.7}$$

where $\boldsymbol{e}_y$ is the unit vector directed along the y-axis and

$$\boldsymbol{n}_\pm = \pm\frac{1}{\sqrt{1 + \left(\dfrac{\partial x_\pm}{\partial y}\right)^2}}\begin{bmatrix} 1 \\ \dfrac{\partial x_\pm}{\partial y} \end{bmatrix} \tag{2.8}$$

are the unit outward normals to the contact lines. Finally, we require that

$$\boldsymbol{v}_\pm \cdot \boldsymbol{n}_\pm = V(\theta_\pm), \tag{2.9}$$

where

$$\boldsymbol{v}_\pm = \begin{bmatrix} \dfrac{\partial x_\pm}{\partial t} \\ 0 \end{bmatrix}, \qquad \theta_\pm = \mp\boldsymbol{n}_\pm \cdot (\nabla h)_{x \to x_\pm}, \tag{2.10}$$

and $V(\theta)$ is a given function determined by the material properties of the liquid and substrate. Note that the left-hand side of (2.9) represents the normal component of the velocity of the contact lines, and $\theta_\pm$ are the contact angles. Subject to initial conditions, set (2.4), (2.6)–(2.10) fully describes the unknowns $h(x, y, t)$ and $x_\pm(y, t)$.

Consider a steady rivulet bounded by two straight lines, described by

$$h = \bar{h}(x), \qquad x_\pm = \pm x_0, \tag{2.11}$$

where x_0 is the rivulet's half-width. For this solution, the governing equations yield $\bar{h} = A(\cosh x_0 - \cosh x)$, where A is an arbitrary constant. Without a loss of generality, one can put $A = (\cosh x_0 - 1)^{-1}$, i.e.

$$\bar{h} = \frac{\cosh x_0 - \cosh x}{\cosh x_0 - 1}. \tag{2.12}$$

Now, the maximum of $\bar{h}(x)$ is equal to unity, which makes the scale H [used in non-dimensionalization (2.2)–(2.3)] the rivulet's dimensional depth. Note that the contact angles corresponding to solution (2.12) are equal and uniquely related to the rivulet's width

$$\theta_\pm = \theta_0 = \frac{\sinh x_0}{\cosh x_0 - 1}. \tag{2.13}$$

Finally, to ensure that the contact lines are stationary, one should require

$$V(\theta_0) = 0$$

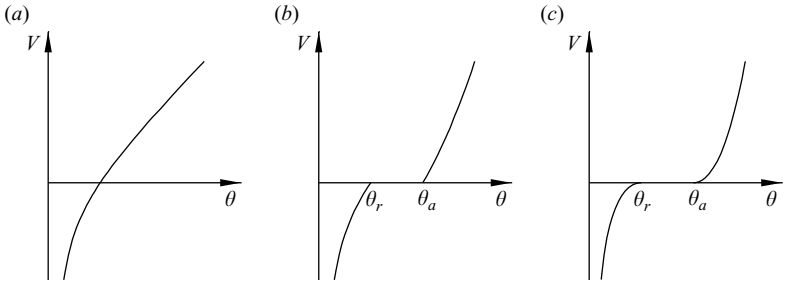

FIGURE 2. Examples of the dependence of the contact-line velocity V on the contact angle θ: (*a*) $V(\theta)$ involves a single equilibrium value of θ; (*b*) $V(\theta)$ involves an hysteresis interval $[\theta_r, \theta_a]$, such that the derivative $\mathrm{d}V/\mathrm{d}\theta$ does not exist at its endpoints; (*c*) $V(\theta)$ involves an hysteresis interval, such that $\mathrm{d}V/\mathrm{d}\theta = 0$ at $\theta = \theta_r, \theta_a$.

(formally, this condition follows from (2.9)). Thus, if the function $V(\theta)$ is as shown in figure 2(*a*), steady rivulets exist for a single value of x_0 – whereas, for $V(\theta)$ shown in figures 2(*b*) and 2(*c*), rivulets exist in a certain interval of x_0 (such that the corresponding range of θ_0 coincides with the hysteresis interval).

In order to examine the stability of solution (2.12), assume that

$$h = \bar{h}(x) + \tilde{h}(x, y, t), \qquad x_\pm = \pm x_0 + \tilde{x}_\pm(y, t), \tag{2.14}$$

where $\tilde{h}$ and $\tilde{x}_\pm$ describe a small disturbance. Substituting (2.14) into (2.4) and linearizing, we obtain

$$\frac{\partial \tilde{h}}{\partial t} + \gamma \frac{\partial}{\partial y}\left(\bar{h}^2\tilde{h} + 2\mu\bar{h}\tilde{h}\right) + \nabla\cdot\left[\left(\frac{\bar{h}^3}{3} + \mu\bar{h}^2\right)\nabla\left(\nabla^2\tilde{h} - \tilde{h}\right)\right] = 0. \tag{2.15}$$

The linearization of the boundary conditions (2.6)–(2.10) is slightly less straightforward, as it implies 'extrapolating' them from the perturbed positions of the contact lines to the unperturbed ones. Rewriting, for example, condition (2.6) in the form

$$\bar{h}(\pm x_0 + \tilde{x}_\pm) + \tilde{h}(\pm x_0 + \tilde{x}_\pm, y, t) = 0,$$

we expand it in powers of $\tilde{x}$ and take into account linear terms only, which yields

$$\frac{\mathrm{d}\bar{h}}{\mathrm{d}x}\tilde{x}_\pm + \tilde{h} \to 0 \qquad \text{as} \qquad x \to \pm x_0. \tag{2.16}$$

Processing in the same manner conditions (2.7)–(2.10), we obtain

$$\left(\frac{\bar{h}^3}{3} + \mu\bar{h}^2\right)\frac{\partial}{\partial x}\left(\nabla^2\tilde{h} - \tilde{h}\right) \to 0 \qquad \text{as} \qquad x \to x_\pm, \tag{2.17}$$

$$\frac{\mathrm{d}\tilde{x}_\pm}{\mathrm{d}t} = V_0'\left(\frac{\partial\tilde{h}}{\partial x} + \frac{\mathrm{d}^2\bar{h}}{\mathrm{d}x^2}\tilde{x}_\pm\right)_{x\to\pm x_0}, \tag{2.18}$$

where

$$V_0' = \left(\frac{\mathrm{d}V}{\mathrm{d}\theta}\right)_{\theta=\theta_0}.$$

This work will be confined to disturbances with harmonic dependence on t and y (normal modes),

$$\tilde{h}(x, y, t) = \phi(x)\,\mathrm{e}^{st+\mathrm{i}ky}, \qquad \tilde{x}_\pm = \eta_\pm\,\mathrm{e}^{st+\mathrm{i}ky}, \tag{2.19}$$

where $\mathrm{Im}\, s$ is the disturbance's frequency, $\mathrm{Re}\, s$ is its growth/decay rate, k is the wavenumber and $\phi(x)$ describes the transverse structure of the disturbance. Substitution of (2.19) into (2.15)–(2.18) yields

$$s\phi + \mathrm{i}\gamma k\bar{h}^2\phi + \frac{\mathrm{d}}{\mathrm{d}x}\left[\left(\frac{\bar{h}^3}{3} + \mu\bar{h}^2\right)\frac{\mathrm{d}}{\mathrm{d}x}\left(\frac{\mathrm{d}^2\phi}{\mathrm{d}x^2} - k^2\phi - \phi\right)\right] - k^2\left(\frac{\bar{h}^3}{3} + \mu\bar{h}^2\right)\left(\frac{\mathrm{d}^2\phi}{\mathrm{d}x^2} - k^2\phi - \phi\right) = 0, \quad (2.20)$$

$$\phi + \frac{\mathrm{d}\bar{h}}{\mathrm{d}x}\eta_\pm \to 0 \qquad \text{as} \qquad x \to \pm x_0, \quad (2.21)$$

$$\left(\frac{\bar{h}^3}{3} + \mu\bar{h}^2\right)\frac{\mathrm{d}}{\mathrm{d}x}\left(\frac{\mathrm{d}^2\phi}{\mathrm{d}x^2} - k^2\phi - \phi\right) \to 0 \qquad \text{as} \qquad x \to \pm x_0, \quad (2.22)$$

$$s\eta_\pm = V_0'\left(\frac{\mathrm{d}\phi}{\mathrm{d}x} + \frac{\mathrm{d}^2\bar{h}}{\mathrm{d}x^2}\eta_\pm\right) \qquad \text{as} \qquad x \to \pm x_0. \quad (2.23)$$

Equations (2.20)–(2.23) form an eigenproblem, where ϕ and s are the eigenfunction and eigenvalue. If there exists a wavenumber k such that one or more eigenvalues have positive real parts, $\mathrm{Re}\, s > 0$, the rivulet is unstable.

2.2. *How do contact lines affect linear stability of liquid films?*

Observe that the only characteristic of the contact-line dynamics that appears in our stability problem is the derivative V_0' of the contact-line velocity evaluated at the equilibrium contact angle. Thus, to answer the title question of this subsection, one needs to examine the structure of the function $V(\theta)$ near $\theta = \theta_0$.

Note that, for most liquid–substrate combinations, $V(\theta)$ involves a hysteresis interval (e.g. Extrand 2006) – i.e. for all $\theta < \theta_r$, the contact line recedes; for $\theta > \theta_a$, it advances; and for $\theta_r \leqslant \theta \leqslant \theta_a$, it is stationary. Accordingly, the equilibrium contact angle θ_0 can assume any of the hysteresis values (in other words, the hysteresis interval can as well be called the equilibrium interval).

Next, observe that, for all hysteresis/equilibrium values in the example shown in figure 2(*c*),

$$V_0' = 0.$$

As a result, the boundary conditions (2.23) yield $\eta_- = \eta_+ = 0$, i.e. the contact lines in this case are fixed (pinned to the substrate). We emphasize that the above statement is not an *assumption*, but a *conclusion* resulting from the existence of an hysteresis interval and smallness of the disturbance's amplitude. We note also that this conclusion could have been deduced from the 'Note added in proof' and equation (5.10*a*) of the paper by Davis (1980).

Moreover, one can arrive at the same conclusion through the following qualitative argument: consider a drop of liquid on a plate which is being shaken by external forcing. Our everyday experience suggests that, if the liquid is not perfectly wetting and the plate's oscillations are sufficiently weak, the drop would remain in its original position. The same should hold if the external forcing is replaced with a sufficiently weak 'internal' (self-generated) disturbance – and, finally, if the drop is replaced with a rivulet. In other words, when examining *linear* stability of liquids *with hysteresis intervals* (be that drops or rivulets) one can safely assume the contact lines to be fixed.

A similar conclusion can be drawn for the example shown in figure 2(*b*) (except for the cases where $\theta_0 = \theta_r, \theta_a$, for which the derivative V_0' does not exist, i.e. the problem cannot be treated through linearization). Finally, the example in figure 2(*a*) does not involve an hysteresis interval – in which case $V_0' \neq 0$, and the contact lines can move (the stability of rivulets for this model has been examined by Wilson & Duffy 1998; Sullivan *et al.* 2008).

In this paper, we shall confine ourselves to the cases where the dependence of the contact-line velocity on the contact angle involves a hysteresis interval, and the rivulet's contact angle θ_0 is strictly inside it (not on its boundary). In this case, we can safely assume $V_0' = 0$, and the stability eigenproblem (2.20)–(2.23) reduces to

$$s\phi + \mathrm{i}\gamma k\bar{h}^2\phi + \frac{\mathrm{d}}{\mathrm{d}x}\left[\frac{\bar{h}^3}{3}\frac{\mathrm{d}}{\mathrm{d}x}\left(\frac{\mathrm{d}^2\phi}{\mathrm{d}x^2} - k^2\phi - \phi\right)\right] - k^2\left(\frac{\mathrm{d}^2\phi}{\mathrm{d}x^2} - k^2\phi - \phi\right) = 0, \quad (2.24)$$

$$\phi \to 0, \qquad \frac{\bar{h}^3}{3}\frac{\mathrm{d}}{\mathrm{d}x}\left(\frac{\mathrm{d}^2\phi}{\mathrm{d}x^2} - k^2\phi - \phi\right) \to 0 \qquad \text{as} \qquad x \to \pm x_0. \quad (2.25)$$

Observe also that, since the contact lines no longer move, the terms involving the non-dimensional slip length μ have been omitted. This affects the solution only in a region where $h \lesssim \mu$, which is extremely narrow (as, typically, $\mu \lesssim 10^{-5}$).

2.3. *A proof of stability of all rivulets on a plate*

Multiply (2.24) by

$$\left(\frac{\mathrm{d}^2\phi}{\mathrm{d}x^2} - k^2\phi - \phi\right)^*$$

(where the asterisk denotes complex conjugation) and integrate with respect to x from $-x_0$ to x_0. Integrating by parts and using the boundary conditions (2.25), one can obtain

$$sI_1 = I_2 + \mathrm{i}I_3, \quad (2.26)$$

where

$$I_1 = -\int_{-x_0}^{x_0}\left(\left|\frac{\mathrm{d}\phi}{\mathrm{d}x}\right|^2 + k^2|\phi|^2 + |\phi|^2\right)\mathrm{d}x,$$

$$I_2 = \int_{-x_0}^{x_0}\frac{\bar{h}^3}{3}\left[\left|\frac{\mathrm{d}}{\mathrm{d}x}\left(\frac{\mathrm{d}^2\phi}{\mathrm{d}x^2} - k^2\phi - \phi\right)\right|^2 + k^2\left|\frac{\mathrm{d}^2\phi}{\mathrm{d}x^2} - k^2\phi - \phi\right|^2\right]\mathrm{d}x,$$

$$I_3 = \gamma k\int_{-x_0}^{x_0}\bar{h}^2\left(\left|\frac{\mathrm{d}\phi}{\mathrm{d}x}\right|^2 + k^2|\phi|^2 + |\phi|^2\right)\mathrm{d}x.$$

Then, it follows from (2.26) that $\mathrm{Re}\, s < 0$ – hence, all rivulets are stable with respect to all disturbances regardless of their wavenumbers. Observe also that the phase velocity $\mathrm{Im}\, s/k$ is positive, i.e. all disturbances propagate downstream.

2.4. *Discussion*

(*a*) Recall that all our results have been obtained using the lubrication approximation, which does not take into account inertia (described by the material derivatives in the Navier–Stokes equations). Generally, inertia can be a destabilizing effect (e.g. Benilov & O'Brien 2005) – but, even if it does cause instability in the

problem at hand, it should be weak (as it scales with the Reynolds number, which is small).

(*b*) Methodologically, our approach is closest to the normal-mode analysis of Davis (1980) and Weiland & Davis (1981). The latter work showed that, if the Reynolds number is below a certain threshold (proportional to the Bond number), a shallow rivulet with fixed contact lines is stable with respect to long-wave disturbances (such that their wavelengths are much larger than the rivulet's width). To draw a connection between this conclusion and our results, observe that the lubrication approximation (which was used to derive our main governing equation (2.1)) implies that the corresponding Reynolds number is small, whereas the Bond number is order-one, so the criterion of Weiland & Davis (1981) holds automatically – hence, long-wave disturbances are certainly stable.

Our results in the previous subsection extend the conclusion of Weiland & Davis (1981) to disturbances with *arbitrary* wavelengths and, thus, prove the *overall* stability of shallow rivulets on a plate.

(*c*) It is less clear how our results can be compared to those of Schmuki & Laso (1990) who showed that, in some cases, it is energetically favourable for a rivulet on a sloping plate to break up into several smaller subrivulets. However, even though a single large rivulet does not correspond to the absolute minimum of energy, it can still correspond to a local one, in which case small disturbances are not capable of destabilizing it. Moreover, since energy is not conserved in viscous fluids and an Arnold-style analysis of conservation laws is impossible, it is not immediately clear how energy is connected to the behaviour of disturbances.

3. Rivulets on the underside of a plate

Rivulets on the underside of a plate are described by (2.1) with $\alpha > \pi/2$. Then, to non-dimensionalize (2.1), one should modify the definition (2.3) of the capillary length L_c,

$$L_c = \sqrt{-\frac{\sigma}{\rho g \cos\alpha}},$$

and eventually obtain the following non-dimensional equation:

$$\frac{\partial h}{\partial t} + \gamma \frac{\partial}{\partial y}\left(\frac{h^3}{3} + \mu h^2\right) + \nabla\cdot\left[\left(\frac{h^3}{3} + \mu h^2\right)\nabla\left(\nabla^2 h + h\right)\right] = 0,$$

which differs from (2.4) by the last term's sign. Then, steady-state rivulets on the underside of a plate are described by

$$\bar{h} = \frac{\cos x - \cos x_0}{1 - \cos x_0}, \tag{3.1}$$

and the stability eigenvalue problem (the equivalent of (2.24)–(2.25)) has the form

$$s\phi + \mathrm{i}\gamma k \bar{h}^2 \phi + \frac{\mathrm{d}}{\mathrm{d}x}\left[\frac{\bar{h}^3}{3}\frac{\mathrm{d}}{\mathrm{d}x}\left(\frac{\mathrm{d}^2\phi}{\mathrm{d}x^2} - k^2\phi + \phi\right)\right] - k^2\left(\frac{\mathrm{d}^2\phi}{\mathrm{d}x^2} - k^2\phi + \phi\right) = 0, \tag{3.2}$$

$$\phi \to 0, \qquad \frac{\bar{h}^3}{3}\frac{\mathrm{d}}{\mathrm{d}x}\left(\frac{\mathrm{d}^2\phi}{\mathrm{d}x^2} - k^2\phi + \phi\right) \to 0 \qquad \text{as} \qquad x \to \pm x_0. \tag{3.3}$$

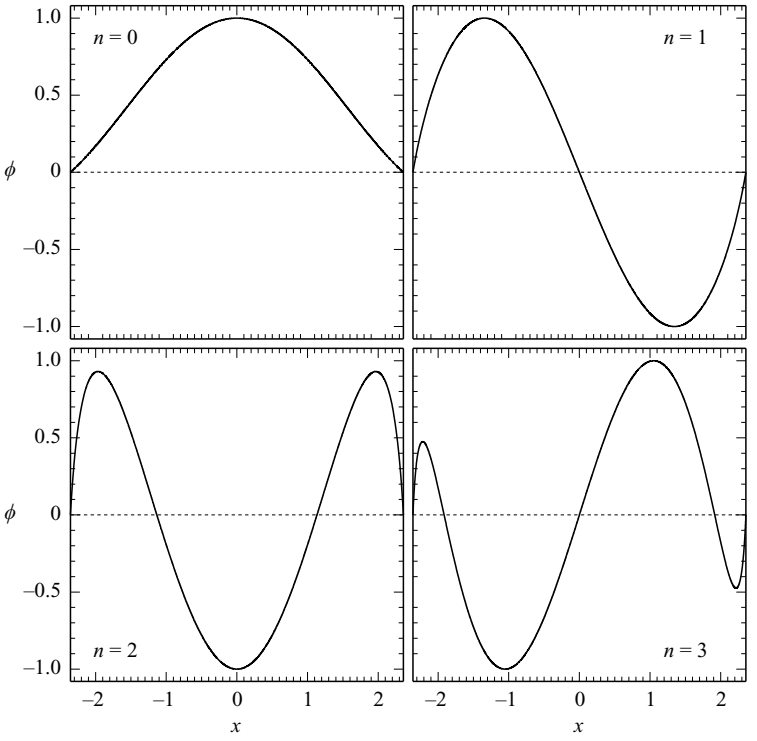

FIGURE 3. Eigenfunctions for the case of horizontal plate (eigenproblem (3.4), (3.3)), for $x_0 = 3\pi/4$, $k = 0$. The panels are labelled with the corresponding modenumbers n (which evidently coincides with the number of ϕ's zeros at internal points of the interval $(-x_0, x_0)$).

In the next two subsections, we shall study (numerically and analytically) the case of horizontal plate, $\gamma = 0$. Then, using it as a 'foothold', we shall examine the general case, $\gamma \neq 0$, in § 3.3.

3.1. *The case of a horizontal plate: numerical results*

Let the plate's slope be zero. Accordingly, $\gamma = 0$, and (3.2) becomes

$$s\phi + \frac{\mathrm{d}}{\mathrm{d}x}\left[\frac{\bar{h}^3}{3}\frac{\mathrm{d}}{\mathrm{d}x}\left(\frac{\mathrm{d}^2\phi}{\mathrm{d}x^2} - k^2\phi + \phi\right)\right] - \frac{k^2\bar{h}^3}{3}\left(\frac{\mathrm{d}^2\phi}{\mathrm{d}x^2} - k^2\phi + \phi\right) = 0. \qquad (3.4)$$

In this subsection, eigenproblem (3.4), (3.3) will be examined numerically (using the approach described in Appendix A).

It turns out that, for all allowable x_0, problem (3.4), (3.3) admits an infinite sequence of real eigenvalues. When numbering them, it is convenient to assign the zero number, $n = 0$, to the largest eigenvalue; $n = 1$, to the second largest one, *etc*. The corresponding eigenfunctions are shown in figure 3, which suggests that a kind of Sturm Oscillation and Comparison Theorem holds in the problem at hand: the eigenfunction with $n = 0$ (zeroth mode) does not have roots at internal points of the interval $(-x_0, x_0)$, the first mode has one root, *etc*. Observe also that, due to the symmetry of the problem, even-numbered eigenfunctions are even and odd-numbered ones are odd.

The dependence of the eigenvalue s on the wavenumber k, i.e. *the dispersion relation*, is illustrated in figure 4: evidently, this particular rivulet is unstable with respect to disturbances of the zeroth mode, $n = 0$.

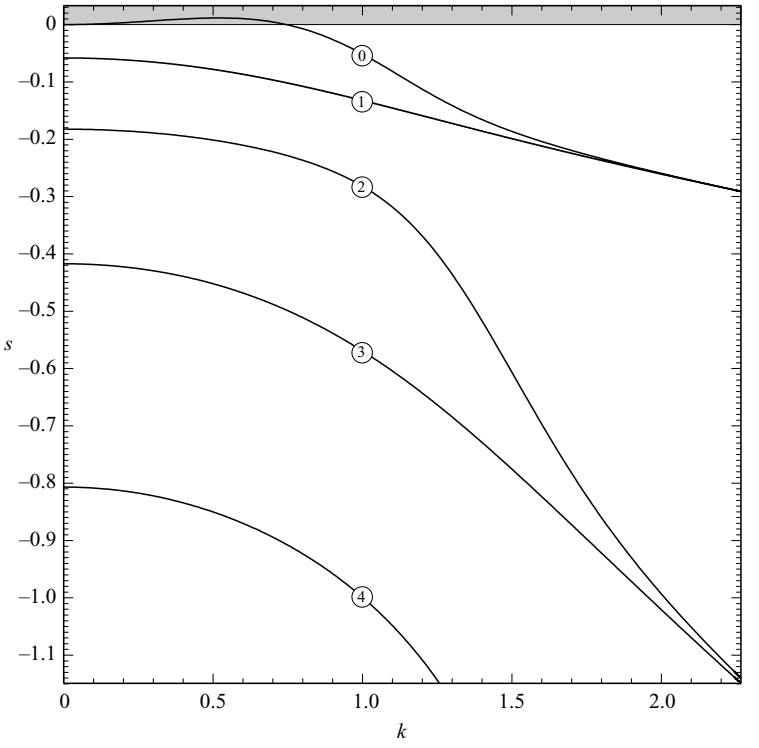

FIGURE 4. The dispersion curves (eigenvalues s versus wavenumber k) for the case of horizontal plate and $x_0 = 3\pi/4$. The curves are labelled with the corresponding modenumbers n. The instability region $s > 0$ is shaded.

In fact, the zeroth mode has turned out to be the only unstable mode in the problem: given that, for $n = 0$, $\phi(x)$ looks pretty much like the profile $\bar{h}(x)$ of the rivulet itself, we conclude that the instability has a modulational nature. Indeed, since the 'full' disturbance (given by (2.19)) oscillates with y, one can see that the zeroth mode causes periodic modulations of the rivulet's amplitude in the down-the-stream direction. One can assume that, once the the modulations become comparable to the depth of the rivulet, it will break up into separate pendant drops.

Observe also the 'mergers' of even- and odd-numbered dispersion curves as $k \to \infty$. In this limit, the eigenfunctions become localized near the endpoints of the interval $(-x_0, x_0)$ (see figure 5), with two consecutive eigenfunctions almost coinciding in one half of the interval and being opposite in sign (but still very close in magnitude) in the other half (see figure 6). At the same time, the eigenvalues corresponding to such eigenfunctions become very close, and the two dispersion curve merge.

Examples considered for narrower rivulets suggest that the instability disappears for some threshold value of x_0, and all dispersion curves are all located in the stable semiplane $s \leqslant 0$. Increasing x_0, on the other hand, strengthens instability (see figure 7), i.e. wider rivulets are more unstable than narrower ones.

In the next subsection, the above conclusion will be quantified. It will be shown that rivulets with $x_0 \leqslant \pi/2$ are stable, and those with $x_0 > \pi/2$ are unstable.

3.2. *The case of a horizontal plate: analytical results*

In this subsection, we shall outline a 'chain' of theorems proving that $x_0 = \pi/2$ is the threshold separating stable and unstable rivulets. The proofs are presented in Appendix B.

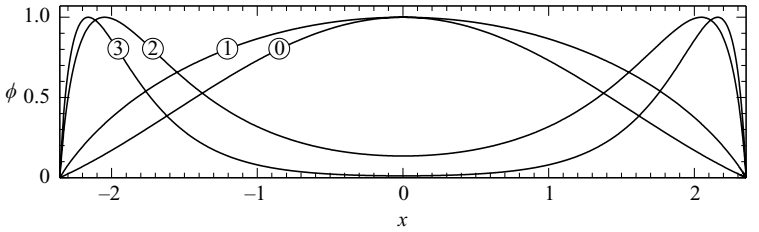

FIGURE 5. The dependence of the zeroth ($n=0$) eigenfunction on k, for the case of horizontal plate and $x_0=3\pi/4$. The curves are labelled with the corresponding values of k. Observe that, with increasing k, the curves become localized near the endpoints of the interval.

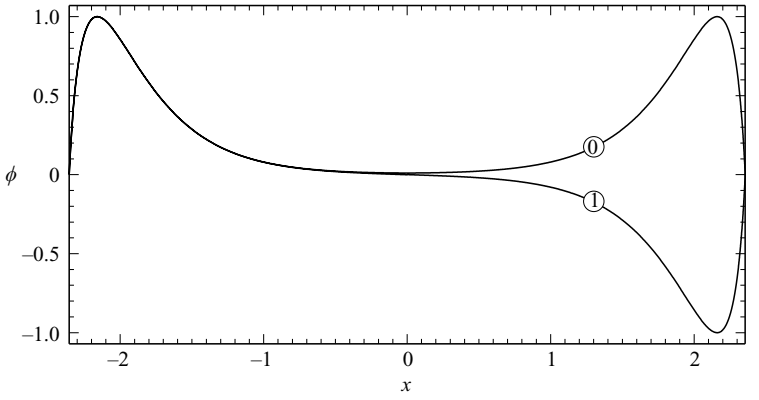

FIGURE 6. The zeroth and first modes for the case of horizontal plate and $k=3$, $x_0=3\pi/4$. The curves are labelled with the corresponding modenumbers.

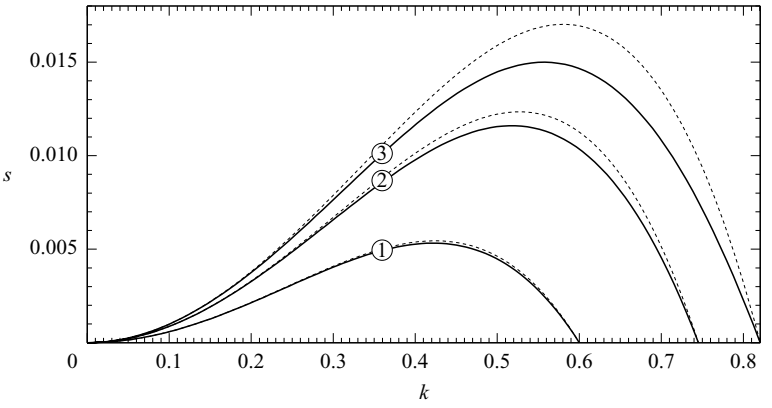

FIGURE 7. The growth rate s versus wavenumber k for the case of horizontal plate. (a) $x_0=5\pi/8$, (b) $x_0=6\pi/8$, (c) $x_0=7\pi/8$. The dotted line corresponds to the approximate formulae (B 18), (B 17) (see Appendix B).

The starting theorem of the 'chain' is as follows:

T1: All eigenvalues of problem (3.4), (3.3) are real.

This conclusion focuses one's attention on those values of k for which $s=0$, as they are the only ones where a dispersion curve $s(k)$ can cross from the stable semiplane $s\leqslant 0$ into the unstable semiplane $s>0$.

T2: If $x_0 \leqslant \pi/2$, *problem (3.4), (3.3) has zero eigenvalues only for* $k^2 = 0$. *If* $x_0 > \pi/2$, *there are two such points:* $k^2 = 0$ *and*

$$k^2 = 1 - \frac{\pi^2}{4x_0^2}. \tag{3.5}$$

This result is particularly important for $x_0 \leqslant 1/2\pi$ – in this case, dispersion curves are either fully stable or fully unstable, as they cannot cross the line $s = 0$ for any $k^2 > 0$. Accordingly, if one shows that all dispersion curves are 'negative' (stable) for *some* k^2, this would amount to stability for *all* k^2.

T3: If $x_0 \leqslant \pi/2$, *all dispersion curves tend to minus-infinity in the short-wave limit, i.e.*

$$s \to -\infty \qquad \text{as} \qquad k^2 \to \infty.$$

Together with T2, this result proves that rivulets with $x_0 \leqslant \pi/2$ are all stable. The stability properties of wider rivulets are still unclear.

T4: Let s' *be the derivative of an eigenvalue with respect to* k^2. *Then, if* $x_0 > \pi/2$, *there exists a solution such that*

$$s = 0, \qquad s' > 0 \qquad \text{for} \qquad k^2 = 0.$$

This result guarantees that, if $x_0 > \pi/2$, the dispersion curve of one of the modes is 'positive' (unstable) in a certain region near $k^2 = 0$. Even if $s(k)$ eventually crosses into the negative semiplane (which it indeed does – see figure 4), the corresponding rivulet is still unstable.

3.3. *The case of a sloping plate*

A non-zero slope of the plate induces in a rivulet a sheared flow, and sheared flows are usually viewed as a source of instability. In the problem at hand, however, they turn out to be a *stabilizing* factor!

Unfortunately, few analytical results can be obtained for $\gamma \neq 0$ – therefore, the above conclusion is mainly supported by numerical evidence. Generally, one just needs to compute the neutral stability curve on the (x_0, γ) plane – to do so, we employed the method described in Appendix A, and the results are presented in figure 8. One can see that, if the slope is sufficiently large,

$$\gamma \gtrsim 0.835, \tag{3.6}$$

all rivulets are stable regardless of their widths.

Also, observe the 'tick' on the neutral stability curve which subdivides it into two parts – these parts correspond to different 'patterns' of stabilization with growing γ. If we are increasing γ for $x_0 \lesssim 2.36$, the last pocket of instability will be located near $k = 0$ (see figure 9*a*) – whereas, for larger x_0, it will be located at medium wavenumbers (see figure 9*b*). The latter circumstance is the main reason why the stability criterion obtained for $\gamma = 0$ (and based on the analysis of the dispersion curve at $k^2 = 0$) cannot be extended to the general case.

In addition, the two patterns of stabilization correspond to two different behaviours of marginally unstable rivulets. Consider, for example, an (x_0, γ) pair just below the (*a*) part of the marginal stability curve in figure 8. Since the corresponding rivulet is unstable with respect to *long*-wave modulations, one can expect it to eventually break up into long/narrow 'segments'. A rivulet with (x_0, γ) just below the (*b*) part of the neutral stability curve, in turn, would break up into drops with *comparable* x and y scales.

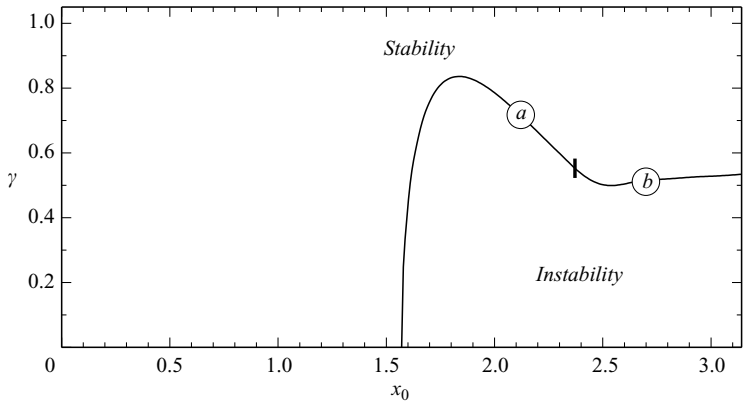

FIGURE 8. The neutral stability curve in the (x_0, γ) parameter space of eigenproblem (3.2)–(3.3) (the rivulet's non-dimensional width x_0 and the substrate's slope γ are linked to the physical parameters by (3.7)). The black vertical 'tick' separates the cases where the transition to stability occurs as in figure 9(a) from the cases where it occurs as in figure 9(b) (the corresponding segments of the neutral stability curve are labelled (a) and (b), respectively).

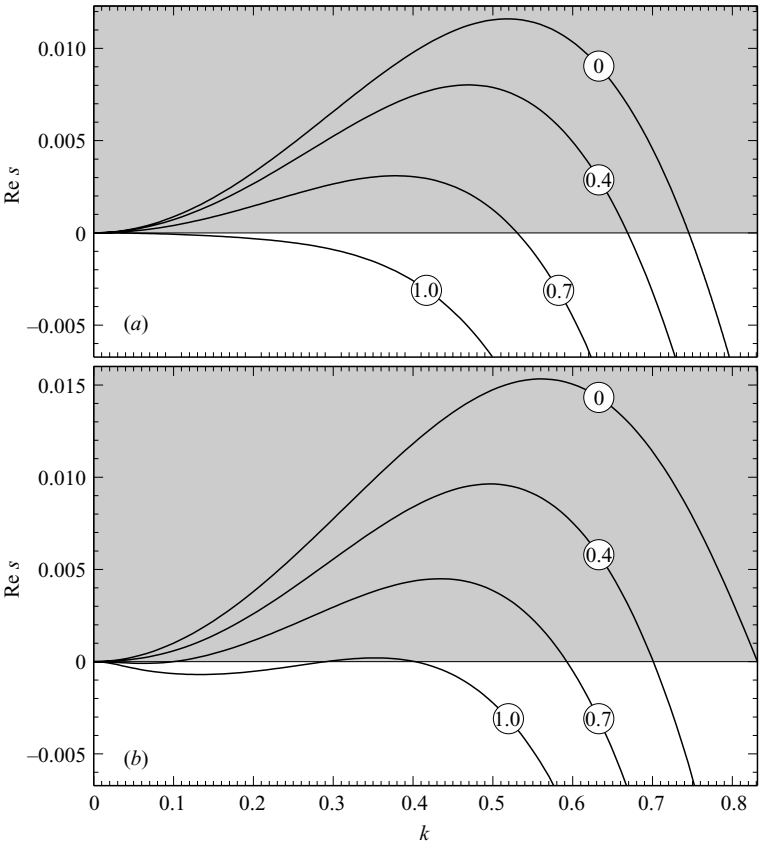

FIGURE 9. The growth/decay rate $\mathrm{Re}\, s$ versus k, for eigenproblem (3.2)–(3.3). The instability region $s > 0$ is shaded. The curves are labelled with the corresponding values of the slope parameter γ. (a) $x_0 = 3\pi/4$, (b) $x_0 = 9\pi/10$. Observe that, in panel (a), the long-wave ($k \to 0$) part of the spectrum becomes stable after all other wavenumbers.

In order to place our results in the 'real-life' context, we shall express x_0 and γ through the dimensional parameters. Recalling how the spatial variables were non-dimensionalized (see (2.2)–(2.3), (2.5)), we obtain

$$x_0 = \frac{W}{2}\sqrt{\frac{\rho g\,\cos\alpha}{\sigma}}, \qquad \gamma = \sqrt{\frac{\sigma}{\rho g\,\cos\alpha}}\frac{\tan\alpha}{H}, \tag{3.7}$$

where W and H are the dimensional width and depth of the rivulet, ρ and σ are the liquid's density and surface tension, α is the angle between the plate and the horizontal and g is the acceleration due to gravity.

Now our results can be illustrated physically. Let the liquid under consideration be water, for which

$$\rho \approx 1000\,\mathrm{kg\,m^{-3}}, \qquad \sigma \approx 0.073\,\mathrm{N\,m^{-1}}.$$

Recalling that, for the case of horizontal plate $\alpha = 0$, all rivulets with $x_0 \leqslant \pi/2$ are stable, one can use the first equality of (3.7) to obtain a stability condition for the rivulet's dimensional width,

$$W \lesssim 8.6\,\mathrm{mm}.$$

Next, let the dimensional depth of the rivulet be

$$H = 0.5\,\mathrm{mm}.$$

Then, using the second equality of (3.7), one can see that the stability condition (3.6) corresponds to

$$\alpha \gtrsim 8.7^\circ.$$

This example shows that rivulets can be stabilized by a fairly mild slope of the substrate.

Finally, note that, instead of x_0, all of our results can be formulated in terms of the rivulet's contact angle θ_0 (as the two parameters are related by (2.13)). It is more instructive, however, to draw the neutral stability curve on the (x_0, τ) plane, where

$$\tau = \frac{2H/W}{\tan\alpha} \tag{3.8}$$

is the 'transverse' slope of the the rivulet's surface, normalized by the plate's slope. This neutral stability curve is presented in figure 10: observe that instability occurs only if τ is sufficiently large. Indeed, given that the slope of a liquid's surface is a measure of nonlinearity – and nonlinear effects are, generally, the underlying cause of instabilities – it comes as no surprise that rivulets with sufficiently large τ are unstable. Furthermore, this conclusion helps to 'come to terms' with the stabilizing nature of the substrate's slope, as an increase in $\tan\alpha$ reduces τ (and, thus, brings it inside the stability region).

4. Summary and concluding remarks

Thus, we examined the linear stability of rivulets. First, we proved that all rivulets on a sloping plate are stable and, second, computed a stability criterion for rivulets on the underside of a plate. The latter is presented in figure 8 as the neutral stability curve on the (x_0, γ) plane, where x_0 is the rivulet's non-dimensional half-width and γ is the slope parameter, both defined by (3.7). In the case of a horizontal plate, $\gamma = 0$, instability occurs for wide rivulets, such that $x_0 > \pi/2$, whereas the slope was shown to be a stabilizing factor: if sufficiently strong (as in (3.6)), it stabilizes all rivulets regardless of their widths.

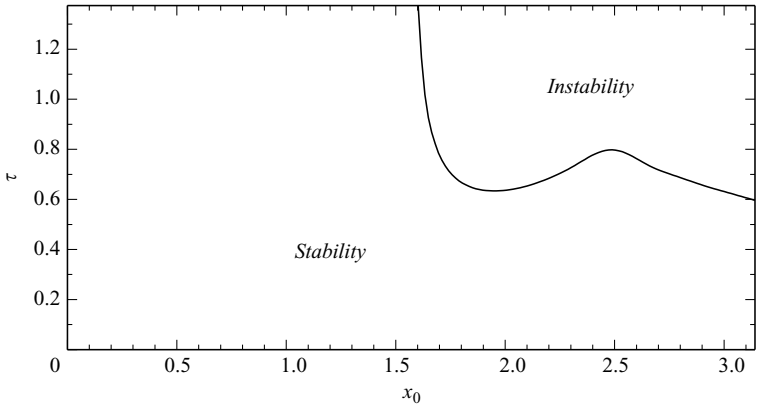

FIGURE 10. The same neutral stability curve as in figure 8, but in the (x_0, τ) parameter space (the rivulet's non-dimensional width x_0 and its slope τ are linked to the physical parameters by (3.7)–(3.8)).

Finally, note that our governing equation (2.1) was derived under the assumption that the effect of inertia (described by the material derivatives in the Navier–Stokes equations) is weak. Generally, inertia is a destabilizing factor (e.g. Benilov & O'Brien 2005), and it would be interesting to explore how it affects the stability of rivulets. Moreover, inertia becomes particularly important when the plate is close to being vertical ($\alpha \approx 90\,^\circ$) – in which case the pressure-gradient term in (2.1) is small, and inertia becomes the main destabilizing factor.

Appendix A. The numerical method for solving (3.2)–(3.3)

Observe that the coefficient of the highest (fourth) derivative in (3.2) involves $\bar{h}^3$ which vanishes at the contact lines. As a result, the points $x = \pm x_0$ – where the boundary conditions (3.3) are set – are singular. In such cases, one can employ a numerical approach used previously by Benilov (2003, 2004) for a similar fourth-order boundary-value problem with singular behaviour at the endpoints (describing the stability of vortices in a two-layer ocean). This approach is based on 'shooting' particular solutions from the endpoints and matching them at an internal point.

To clarify the behaviour of ϕ near, say, $x = -x_0$, introduce ξ such that

$$x = -x_0 + \xi.$$

Then, using Frobenius expansions, one can find the following particular solutions of (3.2):

$$\left.\begin{aligned}
&\phi_1 \to \xi^2 - \frac{s}{6\theta^3}\xi^3 + O(\xi^4)\\
&\phi_2 \to \xi - \frac{3s}{4\theta^3}\xi^2 \ln\xi + O(\xi^3 \ln^2\xi)\\
&\phi_3 \to 1 + \frac{3s}{\theta^3}\xi \ln\xi + O(\xi^2 \ln^2\xi)\\
&\phi_4 \to \ln\xi + \frac{3s}{\theta^3}\xi\left(\tfrac{1}{2}\ln^2\xi - \ln\xi\right) + O(\xi^2 \ln^3\xi)
\end{aligned}\right\} \quad \text{as} \quad \xi \to 0, \qquad \text{(A 1)}$$

where

$$\theta = \left(\frac{\mathrm{d}\bar{h}}{\mathrm{d}x}\right)_{x=-x_0}.$$

Generally, ϕ can be represented in the form

$$\phi = c_1\phi_1 + c_2\phi_2 + c_3\phi_3 + c_4\phi_4,$$

where $c_{1,2,3,4}$ are undetermined constants. One can verify, however, that ϕ_3 and ϕ_4 are inconsistent with the boundary conditions (3.3) – hence, $c_3 = c_4 = 0$, which leaves us with two degrees of freedom (undetermined constants $c_{1,2}$). A similar argument can be applied to the point $x = +x_0$, i.e. there are four degrees of freedom overall. Generally, this is precisely what a fourth-order eigenproblem needs to have a solution.

Now, using the first two of asymptotics (A 1) as initial conditions, one can 'shoot' two linearly independent solutions, $\phi_1^{(-)}$ and $\phi_2^{(-)}$ (the superscript $^{(-)}$ reflects the fact that these solutions originate from $x = -x_0$). $\phi_{1,2}^{(-)}$ can be combined in the form

$$\phi^{(-)} = c_1^{(-)}\phi_1^{(-)} + c_2^{(-)}\phi_2^{(-)}. \tag{A 2}$$

Note that this solution cannot be extended numerically to $x = +x_0$, as this is a singular point of (3.2) and any numerical methods would fail near it.

Next, we compute $\phi_1^{(+)}$ and $\phi_2^{(+)}$ (where the $^{(+)}$ implies that these solutions originate from $x = +x_0$) and combine them to obtain

$$\phi^{(+)} = c_1^{(+)}\phi_1^{(+)} + c_2^{(+)}\phi_2^{(+)}. \tag{A 3}$$

Now, assume that s is an eigenvalue – in which case a global solution, satisfying all boundary conditions, must exist. Accordingly, solutions (A 2) and (A 3) – as well as their first, second and third derivatives – can be required to match at any internal point x_i,

$$\left.\begin{aligned}
c_1^{(-)}\phi_1^{(-)} + c_2^{(-)}\phi_2^{(-)} &= c_1^{(+)}\phi_1^{(+)} + c_2^{(+)}\phi_1^{(+)} \\
c_1^{(-)}\frac{\mathrm{d}\phi_1^{(-)}}{\mathrm{d}x} + c_2^{(-)}\frac{\mathrm{d}\phi_2^{(-)}}{\mathrm{d}x} &= c_1^{(+)}\frac{\mathrm{d}\phi_1^{(+)}}{\mathrm{d}x} + c_2^{(+)}\frac{\mathrm{d}\phi_1^{(+)}}{\mathrm{d}x} \\
c_1^{(-)}\frac{\mathrm{d}^2\phi_1^{(-)}}{\mathrm{d}x^2} + c_2^{(-)}\frac{\mathrm{d}^2\phi_2^{(-)}}{\mathrm{d}x^2} &= c_1^{(+)}\frac{\mathrm{d}^2\phi_1^{(+)}}{\mathrm{d}x^2} + c_2^{(+)}\frac{\mathrm{d}^2\phi_1^{(+)}}{\mathrm{d}x^2} \\
c_1^{(-)}\frac{\mathrm{d}^3\phi_1^{(-)}}{\mathrm{d}x^3} + c_2^{(-)}\frac{\mathrm{d}^3\phi_2^{(-)}}{\mathrm{d}x^3} &= c_1^{(+)}\frac{\mathrm{d}^3\phi_1^{(+)}}{\mathrm{d}x^3} + c_2^{(+)}\frac{\mathrm{d}^3\phi_1^{(+)}}{\mathrm{d}x^3}
\end{aligned}\right\} \quad \text{at} \quad x = x_i.$$

This should be treated as set of linear homogeneous equations for $c_1^{(-)}$, $c_2^{(-)}$, $c_1^{(+)}$, $c_2^{(+)}$; it has a non-trivial solution only if

$$\det\begin{bmatrix}
\phi_1^{(-)} & \phi_2^{(-)} & -\phi_1^{(+)} & -\phi_1^{(+)} \\
\dfrac{\mathrm{d}\phi_1^{(-)}}{\mathrm{d}x} & \dfrac{\mathrm{d}\phi_2^{(-)}}{\mathrm{d}x} & -\dfrac{\mathrm{d}\phi_1^{(+)}}{\mathrm{d}x} & -\dfrac{\mathrm{d}\phi_1^{(+)}}{\mathrm{d}x} \\
\dfrac{\mathrm{d}^2\phi_1^{(-)}}{\mathrm{d}x^2} & \dfrac{\mathrm{d}^2\phi_2^{(-)}}{\mathrm{d}x^2} & -\dfrac{\mathrm{d}^2\phi_1^{(+)}}{\mathrm{d}x^2} & -\dfrac{\mathrm{d}^2\phi_1^{(+)}}{\mathrm{d}x^2} \\
\dfrac{\mathrm{d}^3\phi_1^{(-)}}{\mathrm{d}x^3} & \dfrac{\mathrm{d}^3\phi_2^{(-)}}{\mathrm{d}x^3} & -\dfrac{\mathrm{d}^3\phi_1^{(+)}}{\mathrm{d}x^3} & -\dfrac{\mathrm{d}^3\phi_1^{(+)}}{\mathrm{d}x^3}
\end{bmatrix} = 0 \quad \text{at} \quad x = x_i. \tag{A 4}$$

Equation (A 4) is, essentially, an equation for the eigenvalue s.

Thus, to compute the eigenvalues of problem (3.2)–(3.3), one should first create a routine (based on, say, the Runge–Kutta method), computing the left-hand side of (A 4) as a function of s. This function should be linked to a root-finding routine (based on, say, the secant method).

Appendix B. Proofs of Theorems T1–T4

(i) To prove T1, multiply (3.4) by

$$\left(\frac{\mathrm{d}^2\phi}{\mathrm{d}x^2} - k^2\phi + \phi\right)^*$$

(where the asterisk denotes complex conjugation) and integrate with respect to x from $-x_0$ to x_0. Integrating by parts and using the boundary conditions (3.3), one can obtain

$$sI_1 = I_2, \tag{B 1}$$

where

$$I_1 = \int_{-x_0}^{x_0} \left(-\left|\frac{\mathrm{d}\phi}{\mathrm{d}x}\right|^2 - k^2|\phi|^2 + |\phi|^2\right) \mathrm{d}x,$$

$$I_2 = \int_{-x_0}^{x_0} \frac{\bar{h}^3}{3} \left[\left|\frac{\mathrm{d}}{\mathrm{d}x}\left(\frac{\mathrm{d}^2\phi}{\mathrm{d}x^2} - k^2\phi + \phi\right)\right|^2 + k^2\left|\frac{\mathrm{d}^2\phi}{\mathrm{d}x^2} - k^2\phi + \phi\right|^2\right] \mathrm{d}x.$$

Clearly, $I_{1,2}$ are both real, but this does not necessarily mean that s is real too, as I_1 can be zero (in which case s can be complex). Note, however, that unless

$$k^2 = 0 \qquad \text{and} \qquad \frac{\mathrm{d}}{\mathrm{d}x}\left(\frac{\mathrm{d}^2\phi}{\mathrm{d}x^2} - k^2\phi + \phi\right) = 0 \qquad \text{for all } x \in (-x_0, x_0), \tag{B 2}$$

or

$$k^2 > 0 \qquad \text{and} \qquad \frac{\mathrm{d}^2\phi}{\mathrm{d}x^2} - k^2\phi + \phi = 0 \qquad \text{for all } x \in (-x_0, x_0), \tag{B 3}$$

I_2 is certainly *non*-zero, and it follows from (B 1) that I_1 is non-zero too. Hence, $s = I_2/I_1$ is real.

If either (B 2) or (B 3) does hold, then $I_2 = 0$ and I_1 can vanish too. However, substitution of either (B 2) or (B 3) into (3.4) yields $s\phi = 0$. Thus, for a non-trivial solution (such that $\phi \neq 0$ for some x), $s = 0$ – which is again real, as required.

(ii) To prove T2, observe that the eigenvalue problem (3.4), (3.3) is satisfied when

$$k^2 = 0, \qquad s = 0, \qquad \phi = \cos x - \cos x_0, \tag{B 4}$$

or

$$k^2 = 1 - \frac{\pi^2}{4x_0^2}, \qquad s = 0, \qquad \phi = \cos kx, \tag{B 5}$$

where the latter solution exists only if $x_0 > \pi/2$ (otherwise $k^2 < 0$). It still remains to prove that no other solution with $s = 0$ exists in the problem.

To do so, consider identity (B 1) with $s = 0$ and observe that it holds only subject to either (B 2) or (B 3). Then, it can be readily shown that the *only* ϕ that satisfies both (B 2) and the boundary conditions (3.3) is given by (B 4), and the *only* solution of (B 3), (3.3) is given by (B 5), as required.

Finally, it is worth mentioning that (B 4) describes an infinitesimal change of the rivulet's amplitude.

(iii) To examine the short-wave ($k^2 \to \infty$) limit of eigenproblem (3.4), (3.3), we shall employ an asymptotic approach developed for similar problems by Simmons (1974), Killworth (1980) and Benilov, Naulin & Rasmussen (2002).

First of all, observe that the large term involving k^4 in (3.4) can only be 'balanced' by the fourth-derivative term, i.e.

$$\frac{\mathrm{d}}{\mathrm{d}x} = \mathrm{O}(k) \qquad \text{as} \qquad k \to \infty. \tag{B 6}$$

Generally, there are two situations where ϕ's derivatives are large: when ϕ is fast oscillating or when it is localized in narrow regions near some points. The former possibility corresponds to the large-modenumber limit, $n \to \infty$ (in which case the problem can be solved asymptotically using the WKB method). In our case, however, n is fixed, and so is the number of ϕ's oscillations – hence, as $k \to \infty$, ϕ becomes more and more localized.

Now we need to find the point(s) of localization, for which there are two possibilities: internal points of the interval $(-x_0, x_0)$ or the endpoints. Numerical examples clearly indicate the latter (see figures 5 and 6), but the safe way to select the localization point(s) is through 'trial and error'.

Assume, accordingly, that the eigenfunction is localized near an internal point $x = x_l$, where

$$\bar{h}(x_l) = \bar{h}_l \neq 0,$$

and expand the coefficients of (3.4) about x_l. Taking into account (B 6) and assuming

$$s = \mathrm{O}(k^4) \qquad \text{as} \qquad k \to \infty$$

(otherwise the eigenvalue drops out of the problem), we keep the leading-order terms only and, thus, obtain

$$s\phi + \frac{\bar{h}_l^3}{3}\frac{\mathrm{d}^2}{\mathrm{d}x^2}\left(\frac{\mathrm{d}^2\phi}{\mathrm{d}x^2} - k^2\phi\right) - \frac{k^2\bar{h}_l^3}{3}\left(\frac{\mathrm{d}^2\phi}{\mathrm{d}x^2} - k^2\phi\right) = 0. \tag{B 7}$$

Since ϕ was assumed to be localized in a small region near x_l, the boundary conditions (3.3) should be 'moved' to infinity,

$$\phi \to 0, \qquad \frac{\bar{h}_l^3}{3}\frac{\mathrm{d}}{\mathrm{d}x}\left(\frac{\mathrm{d}^2\phi}{\mathrm{d}x^2} - k^2\phi\right) \to 0 \qquad \text{as} \qquad x \to \pm\infty. \tag{B 8}$$

The coefficients of (B 7) are constant, which makes it easy to solve – but none of its solutions satisfy the boundary conditions (B 8). We conclude that the localization point(s) can only be located at $x = \pm x_0$.

Consider, for example, $x = -x_0$ and define an 'inner' variable,

$$\hat{\xi} = k\,(x + x_0)\,, \tag{B 9}$$

where the factor k is introduced to make (B 9) consistent with (B 6). It is also convenient to rescale the eigenvalue,

$$\hat{s} = \frac{3s}{\left[\left(\dfrac{\mathrm{d}\bar{h}}{\mathrm{d}x}\right)_{x=-x_0}\right]^3 k}, \tag{B 10}$$

which corresponds to $s = \mathrm{O}(k)$.

Now, expanding (3.4), (3.3) about $x = -x_0$ and taking into account the leading-order terms only, we obtain

$$\hat{s}\phi + \frac{\mathrm{d}}{\mathrm{d}\hat{\xi}}\left[\hat{\xi}^3\frac{\mathrm{d}}{\mathrm{d}\hat{\xi}}\left(\frac{\mathrm{d}^2\phi}{\mathrm{d}\hat{\xi}^2} - \phi\right)\right] - \hat{\xi}^3\left(\frac{\mathrm{d}^2\phi}{\mathrm{d}\hat{\xi}^2} - \phi\right) = 0, \tag{B 11}$$

$$\phi \to 0, \qquad \frac{\hat{\xi}^3}{3}\frac{\mathrm{d}}{\mathrm{d}\hat{\xi}}\left(\frac{\mathrm{d}^2\phi}{\mathrm{d}\hat{\xi}^2} - \phi\right) \to 0 \qquad \text{as} \qquad \hat{\xi} \to 0, +\infty. \tag{B 12}$$

Note that k is implied to be positive here, otherwise the $+\infty$ in (B 12) would be $-\infty$ (see (B 9)).

Now, multiply (B 11) by $\hat{\xi}^{-2}\phi$ and integrate with respect to $\hat{\xi}$ from 0 to $+\infty$ (the convergence of the resulting integrals can be proved by analysing the asymptotics of $\phi(\hat{\xi})$ in a manner similar to (2.14)–(2.16)). Then, integrating where necessary by parts and using the boundary conditions (B 12), one can obtain

$$\hat{s}\int_0^\infty \xi^{-2}\phi^2\,\mathrm{d}\hat{\xi} = -\int_0^\infty \hat{\xi}\left[\left(\frac{\mathrm{d}^2\phi}{\mathrm{d}\hat{\xi}^2}\right)^2 + 2\left(\frac{\mathrm{d}\phi}{\mathrm{d}\hat{\xi}}\right)^2 + \phi^2\right]\mathrm{d}\hat{\xi},$$

which clearly shows that $\hat{s} < 0$. Finally, it follows from (3.1) that

$$\left(\frac{\mathrm{d}\bar{h}}{\mathrm{d}x}\right)_{x=-x_0} > 0,$$

hence, (B 10) implies that s is of the same sign as $\hat{s}$, i.e. negative (stable).

(iv) Observe that solution (B 4) involves a zero eigenvalue s for $k^2 = 0$, which makes it a 'candidate' for T4. It still remains to show that the corresponding s' (the derivative of s with respect to k^2) is positive for $k^2 = 0$.

To do so, differentiate (3.4) and (3.3) with respect to k^2 and substitute $k^2 = 0$, $s = 0$, which yields

$$s'\phi + \frac{\mathrm{d}}{\mathrm{d}x}\left[\frac{\bar{h}^3}{3}\frac{\mathrm{d}}{\mathrm{d}x}\left(\frac{\mathrm{d}^2\phi'}{\mathrm{d}x^2} - \phi + \phi'\right)\right] - \frac{\bar{h}^3}{3}\left(\frac{\mathrm{d}^2\phi}{\mathrm{d}x^2} + \phi\right) = 0, \tag{B 13}$$

$$\phi \to 0, \qquad \frac{\bar{h}^3}{3}\frac{\mathrm{d}}{\mathrm{d}x}\left(\frac{\mathrm{d}^2\phi'}{\mathrm{d}x^2} - \phi + \phi'\right) \to 0 \qquad \text{as} \qquad x \to \pm x_0. \tag{B 14}$$

This boundary-value problem determines ϕ' and s' – but we do not need the former, whereas the latter can be found without solving the whole problem. Indeed, integrating (B 13) with respect to x from $-x_0$ to x_0 and taking into account the second condition in (B 14), one can eliminate ϕ' and obtain

$$s'\int_{-x_0}^{x_0}\phi\,\mathrm{d}x - \int_{-x_0}^{x_0}\frac{\bar{h}^3}{3}\left(\frac{\mathrm{d}^2\phi}{\mathrm{d}x^2} + \phi\right)\mathrm{d}x = 0. \tag{B 15}$$

Now, taking into account the expression for ϕ given by (B 4), one can show that

$$\int_{-x_0}^{x_0}\phi\,\mathrm{d}x > 0, \qquad \int_{-x_0}^{x_0}\frac{\bar{h}^3}{3}\left(\frac{\mathrm{d}^2\phi}{\mathrm{d}x^2} + \phi\right)\mathrm{d}x = -\cos x_0\int_{-x_0}^{x_0}\frac{\bar{h}^3}{3}\mathrm{d}x. \tag{B 16}$$

Together with the obvious inequality $\bar{h} > 0$, conditions (B 15)–(B 16) prove that

$$s' > 0 \qquad \text{for} \qquad x_0 > \tfrac{1}{2}\pi,$$

as required.

Finally, note that (B 15) can be used to obtain an approximate formula for the growth rate of the instability. Substituting (3.1) and (B 12) into (B 15), for $\bar{h}$ and ϕ respectively, and evaluating the integrals involved, we obtain

$$s' = -(\cos x_0)\,\frac{27\,\sin x_0 + 11\,\sin 3x_0 - 6x_0\,(9\,\cos x_0 + \cos 3x_0)}{72\,(\sin x_0 - x_0\,\cos x_0)\,(1-\cos x_0)^3}. \tag{B 17}$$

This expression furnishes us with the value of the derivative of s for $k^2 = 0$. Recall also that, when k^2 is given by (3.5), then $s = 0$. Then, for intermediate values of k^2, one could expect s to be well approximated by

$$s \approx s' k^2 \left(1 - \frac{k^2}{1 - \dfrac{\pi^2}{4x_0^2}} \right). \tag{B 18}$$

The approximate growth rate (B 18), (B 17) and the numerical solution of the exact problem are plotted together in figure 7. One can see that the two results agree reasonably well – especially, for smaller values of x_0.

REFERENCES

Benilov, E. S. 2003 Instability of quasigeostrophic vortices in a two-layer ocean with thin upper layer. *J. Fluid Mech.* **475**, 303–331.

Benilov, E. S. 2004 Stability of vortices in a two-layer ocean with uniform potential vorticity in the lower layer. *J. Fluid Mech.* **502**, 207–232.

Benilov, E. S., Naulin, V. & Rasmussen J. J. 2002 Does a sheared flow stabilize inversely stratified fluid? *Phys. Fluids* **14**, 1674–1680.

Benilov, E. S. & O'Brien, S. B. G. 2005 Inertial instability of a liquid film inside a rotating horizontal cylinder. *Phys. Fluids* **17**, 052106.

Bertozzi, A. L. & Brenner, M. P. 1997 Linear stability and transient growth in driven contact lines. *Phys. Fluids* **9**, 530–539.

Davis, S. H. 1980 Moving contact lines and rivulet instabilities. Part I. The static rivulet. *J. Fluid. Mech.* **98**, 225–242.

Extrand, C. V. 2006 Hysteresis in contact angle measurements. In *Encyclopedia of surface and colloid science,* 2nd edn. (ed. P. Somasundaran & A. T. Hubbard), pp. 2414–2429. Taylor & Francis.

Hocking, L. M. 1981 Sliding and spreading of thin two-dimensional drops. *Quart. J. Mech. Appl. Math.* **34**, 37–55.

Killworth, P. D. 1980 Barotropic and baroclinic instability in rotating fluids. *Dyn. Atmos. Oceans* **4**, 143–184.

Langbein, D. 1990 The shape and stability of liquid menisci at solid edges. *J. Fluid. Mech.* **213**, 251–265.

Myers, T. G., Liang, H. X. & Wetton, B. 2004 The stability and flow of a rivulet driven by interfacial shear and gravity. *Intl J. Nonlinear Mech.* **39**, 1239–1249.

Roy, R. V. & Schwartz, L. W. 1999 On the stability of liquid ridges. *J. Fluid Mech.* **391**, 293–318.

Schmuki, P. & Laso, M. 1990 On the stability of rivulet flow. *J. Fluid Mech.* **215**, 125–143.

Simmons, A. J. 1974 The meridional scale of baroclinic waves. *J. Atmos. Sci.* **31**, 1515–1525.

Sullivan, J. S., Wilson, S. K. & Duffy, B. R. 2008 A thin rivulet of perfectly wetting fluid subject to a longitudinal surface shear stress. *Quart. J. Mech. Appl. Math.* **61**, 25–61.

Weiland, R. H. & Davis, S. H. 1981 Moving contact lines and rivulet instabilities. Part II. Long waves on flat rivulets. *J. Fluid Mech.* **107**, 261–280.

Wilson, S. K. & Duffy, B. R. 1998 On the gravity-driven draining of a rivulet of viscous fluid down a slowly varying substrate with variation transverse to the direction of flow. *Phys. Fluids* **10**, 13–22.

Wilson, S. K. & Duffy, B. R. 2005 When is it energetically favourable for a rivulet of perfectly wetting fluid to split? *Phys. Fluids* **17**, 078104-1–078104-3.